JOURNAL OF GEOPHYSICAL RESEARCH, VOL. 108, NO. C6, 3205, doi:10.1029/2002JC001560, 2003

On the nonlinear integral transform of an ocean wave spectrum into an along-track interferometric synthetic aperture radar image spectrum

Yijun He
Institute of Oceanology, Chinese Academy of Sciences, Qingdao, China

Werner Alpers
Institute of Oceanography, University of Hamburg, Hamburg, Germany

Received 22 July 2002; revised 19 January 2003; accepted 10 April 2003; published 27 June 2003.

[1] We present a new nonlinear integral transform relating the ocean wave spectrum to the along-track interferometric synthetic aperture radar (AT-INSAR) image spectrum. The AT-INSAR, which is a synthetic aperture radar (SAR) employing two antennas displaced along the platform's flight direction, is considered to be a better instrument for imaging ocean waves than the SAR. This is because the AT-INSAR yields the phase spectrum and not only the amplitude spectrum as with the conventional SAR. While the SAR and AT-INSAR amplitude spectra depend strongly on the modulation of the normalized radar cross section (NRCS) by the long ocean waves, which is poorly known, the phase spectrum depends only weakly on this modulation. By measuring the phase difference between the signals received by both antennas, AT-INSAR measures the radial component of the orbital velocity associated with the ocean waves, which is related to the ocean wave height field by a well-known transfer function. The nonlinear integral transform derived in this paper differs from the one previously derived by *Bao et al.* [1999] by an additional term containing the derivative of the radial component of the orbital velocity associated with the long ocean waves. By carrying out numerical simulations, we show that, in general, this additional term cannot be neglected. Furthermore, we present two new quasi-linear approximations to the nonlinear integral transform relating the ocean wave spectrum to the AT-INSAR phase spectrum. *INDEX TERMS:* 4560 Oceanography: Physical: Surface waves and tides (1255); 6924 Radio Science: Interferometry; 6969 Radio Science: Remote sensing; 6959 Radio Science: Radio oceanography; *KEYWORDS:* along-track interferometric synthetic aperture radar, ocean wave, nonlinear transform

Citation: He, Y., and W. Alpers, On the nonlinear integral transform of an ocean wave spectrum into an along-track interferometric synthetic aperture radar image spectrum, *J. Geophys. Res.*, *108*(C6), 3205, doi:10.1029/2002JC001560, 2003.

1. Introduction

[2] The synthetic aperture radar (SAR) is an active microwave instrument which has been widely used to measure ocean surface wave spectra from space. For example, aboard the European Remote Sensing satellites ERS-1 and ERS-2, launched in 1991 and 1995, respectively, and aboard the European Envisat satellite, launched on 1 March 2002, are synthetic aperture radars that have an operating mode specifically designed to measure ocean waves on a global scale. However, retrieving ocean wave spectra from SAR data acquired over the ocean is a nontrivial task [*Hasselmann and Hasselmann*, 1991; *Hasselmann et al.*, 1996; *Heimbach et al.*, 1998]. Owing to the motion of the sea surface, the SAR image represents a highly distorted image of the sea surface [see, e.g., *Alpers and Rufenach*, 1979; *Swift and Wilson*, 1979; *Alpers et al.*, 1981; *Hasselmann et al.*, 1985]. In addition, the modulation of the normalized radar cross section (NRCS) by the ocean wave field also enters into the SAR imaging mechanism. This modulation is poorly known, in particular, the part that results from hydrodynamic modulation of the short surface waves (short gravity waves/capillary waves) by the long ocean waves [*Alpers and Hasselmann*, 1978]. Thus the inversion of SAR image spectra into ocean wave spectra is not only hampered by the nonlinearity of the SAR imaging mechanism induced by the motion of the sea surface (mainly by velocity bunching), but also by the not well known modulation of the NRCS by the long ocean waves. This modulation is sometimes called "real aperture radar (RAR) modulation," because it is this modulation that renders ocean surface waves visible on real aperture radar images.

[3] It has been conjectured that a synthetic aperture radar employing two antennas displaced along the flight direction, called along-track interferometric SAR (AT-INSAR), is

0148-0227/03/2002JC001560

better suited for measuring ocean wave spectra than the conventional SAR employing only one antenna [*Marom et al.*, 1990, 1991; *Lyzenga and Bennett*, 1991]. With an AT-INSAR, one can measure the phase difference between the images from each antenna, which is directly related to the line-of-sight component of the velocity field at the ocean surface. Thus this instrument should be well suited for measuring ocean surface currents [*Goldstein and Zebker*, 1987; *Goldstein et al.*, 1989] as well as ocean surface waves via their orbital motions.

[4] Several papers have been published dealing with the imaging of ocean waves by AT-INAR. The papers of *Shemer and Kit* [1991] and *Shemer* [1995] deal with the imaging of monochromatic waves, while the papers of *Bao et al.* [1997] and *Zilman and Shemer* [1999] deal with the imaging of ocean waves (swell) having a narrow spectrum.

[5] Following *Hasselmann and Hasselmann* [1991] and *Krogstad* [1992], who derived a nonlinear integral transform relating the two-dimensional ocean wave spectrum to the conventional SAR image spectrum, *Bao et al.* [1999] derived a nonlinear integral transform relating this spectrum to the AT-INSAR phase spectrum. However, in their paper a term was neglected that turns out not to be always small. This term is now included in the integral transform derived in this paper.

[6] In addition, we derive also a nonlinear integral transform relating the ocean wave spectrum to the AT-INSAR amplitude spectrum. This transform is almost identical to the nonlinear integral transform derived by *Hasselmann and Hasselmann* [1991] and *Krogstad* [1992] for the conventional SAR. For practical purposes it is of little value because the AT-INSAR amplitude spectrum is not better suited for retrieving ocean wave spectra than the conventional SAR image spectrum. In contrast to this, the AT-INSAR phase spectrum is more useful because it receives information on the ocean waves via the radial component of the orbital velocity. However, there is also a caveat to the AT-INSAR phase spectrum. The measured phase not only contains information on the radial component of the orbital velocity of the scatter element, but also on the displacement of their position in flight direction in the image plane. Thus velocity bunching, which is nonlinear in nature, also contributes to the AT-INSAR phase spectrum. Because of the greater practical value of the AT-INSAR phase spectrum as compared to the AT-INSAR amplitude spectrum, we also derive in this paper two quasi-linear approximations to the nonlinear integral transform relating the ocean wave spectrum to the AT-INSAR phase spectrum.

[7] Finally, for one representative ocean wave spectrum, we compare the results obtained with the transforms derived in this paper with the ones derived by *Bao et al.* [1999] and *Vachon et al.* [1999]. It is shown that the differences are not negligible.

2. AT-INSAR Amplitude and Phase Images

[8] The geometry of the AT-INSAR is depicted schematically in Figure 1. The two AT-INSAR antennas, called fore and aft antennas, are separated by a distance $2B$ in flight direction. Here x_0 denotes the coordinate in flight or along-track direction and y_0 denotes the coordinate in ground range or cross-track direction. The distances from the fore and aft antennas and from the median of the two antennas to

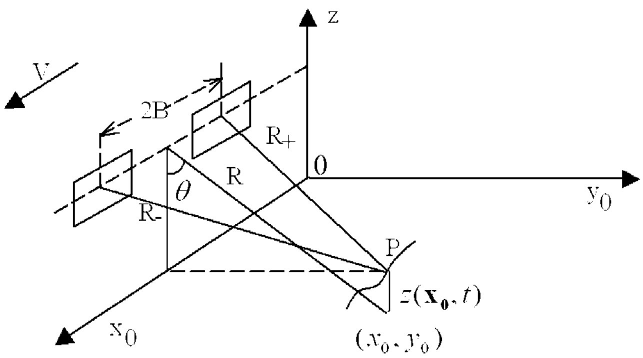

Figure 1. AT-INSAR geometry; the two antennas are displaced in flight direction by 2B.

the scattering element (facet) P on the ocean surface are denoted by R_+, R_-, and R, respectively. The incidence angle is denoted by θ. The fore and aft antennas of the AT-INSAR map an identical scene separated by the time interval $\Delta t = 2B/V$, where V denotes the velocity of the platform carrying the AT-INSAR. The backscattered radar signals from the ocean surface received by the fore and aft antennas are recorded and processed in two separate complex images. These two complex images are then combined into a single complex AT-INSAR image by multiplying the first one by the complex conjugate of the second one.

[9] For the case where only one antenna transmits radar signals and both antennas receive the backscattered signals, *Bao et al.* [1997] have derived the following expression for the complex AT-INSAR image $I(\mathbf{x})$,

$$I(\mathbf{x}) = \frac{\pi}{2} T_0^2 \rho_a \exp\left(-\frac{4B^2}{V^2 T_0^2}\right) \int \frac{\sigma(\mathbf{x}_0)}{\rho'_a(\mathbf{x}_0)} \exp\left[-2jk_i \frac{B}{V} u_r(\mathbf{x}_0)\right] \times \exp\left[\frac{2jBk_i}{R}\left(\frac{2\rho_a^2}{\rho_a'^2(\mathbf{x}_0)} - 1\right)\left(x - x_0 - \frac{R}{V}u_r(\mathbf{x}_0)\right)\right] \times \exp\left[\frac{4\rho_a^2 B^2}{\rho_a'^2(\mathbf{x}_0) T_0^2 V^2} - \frac{\pi^2}{\rho_a'^2(\mathbf{x}_0)}\left(x - x_0 - \frac{R}{V}u_r(\mathbf{x}_0)\right)^2\right] dx_0. \tag{1}$$

Here $\mathbf{x} = (x, y)$ denote the coordinates in the AT-INSAR image plane corresponding to the $\mathbf{x}_0 = (x_0, y_0)$ coordinates in the ocean plane, T_0 denotes the AT-INSAR single look integration time, $\sigma(\mathbf{x}_0)$ denotes the normalized radar cross section (NRCS), $\rho_a = \frac{\lambda_i R}{2VT_0}$ denotes the full-bandwidth single-look azimuthal resolution, $k_i = 2\pi/\lambda_i$, where λ_i is the radar wavelength, $u_r(\mathbf{x}_0)$ denotes the radial (line-of sight) component of the velocity of the scattering element at the sea surface, and $\rho'_a(\mathbf{x}_0)$ denotes the degraded azimuthal resolution, which is given by

$$\rho'_a(\mathbf{x}_0) = \sqrt{\rho_a^2 + \left[\frac{\pi R T_0}{2V} a_r(\mathbf{x}_0)\right]^2 + \frac{\rho_a^2 T_0^2}{\tau_s^2}}, \tag{2}$$

where $a_r(\mathbf{x}_0)$ denotes the radial (line-of-sight) component of the orbital acceleration associated with the ocean wave and τ_s denotes the scene coherence time.

[10] The radial component of the velocity of the scattering element at the sea surface, $u_r(\mathbf{x}_0)$, is the sum of the phase

velocity of the Bragg wave, the radial component of the orbital velocity associated with the long ocean waves, and the radial component of the surface current velocity arising, for example, from wind drift or tidal currents.

[11] The fact that the above expression depends also on the radial component of surface current velocity opens the possibility of also measuring with an AT-INSAR the ocean surface current fields with high spatial resolution. Indeed, the first AT-INSAR was built just for this purpose [*Goldstein and Zebker*, 1987; *Goldstein et al.*, 1989]. However, since we are concerned here with the imaging of ocean surface waves, we retain in our calculations only the spatially variable orbital velocity term $u_r(\mathbf{x}_0)$.

[12] In deriving equation (1) it has been assumed that the SAR impulse function in ground range direction can be approximated by a δ-function and that the SAR integration time T_0 is small compared to the period of the dominant ocean wave. Note that in the AT-INSAR imaging model underlying equation (1) enters the modulation caused by velocity bunching and by radar cross-section modulation as well as the degradation in azimuthal resolution. Two effects contribute to the degradation in azimuthal resolution: (1) the orbital acceleration associated with the long ocean waves and (2) the motion of the scatter elements (facets) within the AT-INSAR resolution cell, which is described by a scene coherence time τ_s. Note, that if we set in equation (1) the distance 2B between the antennas equal to zero, then the phase term in equation (1) vanishes and equation (1) reduces to the well-known expression describing the imaging of ocean waves by a conventional SAR [*Alpers et al.*, 1981; *Brüning et al.*, 1990].

[13] In the following, we shall derive integral transforms which relate the ocean wave spectrum to the AT-INSAR amplitude spectrum as well as to the AT-INSAR phase spectrum. These transforms can only be obtained if we assume that $\rho_a'(\mathbf{x}_0)$ is small compared to the length scale of the long ocean waves. If this is the case then the exponential function,

$$\exp\left\{-\frac{\pi^2}{\rho_a'^2(\mathbf{x}_0)}\left(x - x_0 - \frac{R}{V}u_r(\mathbf{x}_0)\right)^2\right\}, \tag{3}$$

appearing in equation (1) is small everywhere except where

$$x - x_0 - \frac{R}{V}u_r(\mathbf{x}_0) = 0.$$

Thus we may approximate equation (3) by a δ function,

$$\frac{\rho_a'(\mathbf{x}_0)}{\sqrt{\pi}}\delta\left(x - x_0 - \frac{R}{V}u_r(\mathbf{x}_0)\right). \tag{4}$$

Substituting equation (4) into equation (1) and carrying out the integration over x_0, we obtain

$$I(\mathbf{x}) = \frac{\sqrt{\pi}}{2}T_0^2\rho_a\exp\left(-\frac{4B^2}{V^2T_0^2}\right)\left\{\sigma(\mathbf{x}_0)\exp\left[-2jk_i\frac{B}{V}u_r(\mathbf{x}_0)\right]\right.$$
$$\left.\left.\times\exp\left[\frac{4\rho_a^2B^2}{\rho_a'^2(\mathbf{x}_0)T_0^2V^2}\right]\frac{1}{1+\frac{R}{V}u_r'(\mathbf{x}_0)}\right\}\right|_{x_0 = x - \frac{R}{V}u_r(\mathbf{x}_0)} \tag{5}$$

[14] If we assume $1 + \frac{R}{V}u_r'(\mathbf{x}_0) \neq 0$, then the amplitude image and phase images, $I_A(\mathbf{x})$ and $I_P(\mathbf{x})$, respectively, are given by

$$I_A(\mathbf{x}) = \frac{\sqrt{\pi}}{2}T_0^2\rho_a\exp\left(-\frac{4B^2}{V^2T_0^2}\right)\left\{\sigma(\mathbf{x}_0)\times\exp\left[\frac{4\rho_a^2B^2}{\rho_a'^2(\mathbf{x}_0)T_0^2V^2}\right]\right.$$
$$\left.\left.\cdot\frac{1}{1+\frac{R}{V}u_r'(\mathbf{x}_0)}\right\}\right|_{x_0 = x - \frac{R}{V}u_r(\mathbf{x}_0)} \tag{6}$$

$$I_P(\mathbf{x}) = -2k_i\frac{B}{V}u_r(\mathbf{x}_0)\bigg|_{x_0 = x - \frac{R}{V}u_r(\mathbf{x}_0)}. \tag{7}$$

Equation (6) can also be written as

$$I_A(\mathbf{x}) = \frac{\sqrt{\pi}}{2}T_0^2\rho_a\exp\left(-\frac{4B^2}{V^2T_0^2}\right)\int\sigma(\mathbf{x}_0)\exp\left[\frac{4\rho_a^2B^2}{\rho_a'^2(\mathbf{x}_0)T_0^2V^2}\right]$$
$$\times\,\delta\left(x - x_0 - \frac{R}{V}u_r(\mathbf{x}_0)\right)dx_0. \tag{8}$$

[15] If we set $B = 0$, then equation (8) reduces to the corresponding equation (18) of *Hasselmann and Hasselmann* [1991] applicable to a conventional SAR (written, however, in terms of relative image intensity).

[16] Equation (7) can also be written in a similar way as equation (8),

$$I_P(\mathbf{x}) = -2k_i\frac{B}{V}\int u_r(\mathbf{x}_0)\left(1+\frac{R}{V}u_r'(\mathbf{x}_0)\right)\delta\left(x - x_0 - \frac{R}{V}u_r(\mathbf{x}_0)\right)dx_0. \tag{9}$$

[17] Note that equation (8) contains the normalized radar cross section $\sigma_0(\mathbf{x}_0)$ which is modulated by the long ocean waves, while equation (9) depends on the radial component of the orbital velocity $u_r(\mathbf{x}_0)$. In our imaging model we assume that both quantities are related linearly to the wave amplitude. One often refers to the imaging model leading to the transforms (8) and (9) as "pure velocity bunching model," because it is obtained by simply mapping each facet at the azimuthal position x_0 to the corresponding azimuthal position at $x = x_0 + \frac{R}{V}u_r(\mathbf{x}_0)$ in the image plane. This leads to a compression (bunching) and stretching of the originally homogeneous distribution of facets in the image plane. The reader can find a nice illustration of this effect in the paper by *Vachon et al.* [1999, Figures 2 and 3]. Equations (8) and (9) are the mapping functions which we will be used in the next sections to derive the nonlinear transforms relating the ocean wave spectrum to the AT-INSAR amplitude and phase spectra.

[18] Note that the above equation (9) for the AT-INSAR phase image differs from the corresponding equation (6) derived by *Bao et al.* [1999] by the additional term $(R/V)u_r'(\mathbf{x}_0)$. The principal aim of this paper is to show that this term has to be included in the transform.

3. Nonlinear Integral Transform for the AT-INSAR Phase Spectrum

[19] The AT-INSAR phase spectrum $P_p(\mathbf{k})$ is obtained from the AT-INSAR phase image $I_p(\mathbf{x})$ by first calculating the Fourier transform of equation (9),

$$
\begin{aligned}
I_P(\mathbf{k}) &= -k_i \frac{B}{2\pi^2 V} \int\int u_r(\mathbf{x}_0)\left(1 + \frac{R}{V} u'_r(\mathbf{x}_0)\right) \\
&\quad \cdot \delta\left(x - x_0 - \frac{R}{V} u_r(\mathbf{x}_0)\right) dx_0 \, \exp[-j\mathbf{k}\mathbf{x}] d\mathbf{x} \\
&= -k_i \frac{B}{2\pi^2 V} \int h(\mathbf{x}_0) \, \exp[-j\mathbf{k}\mathbf{x}_0] d\mathbf{x}_0, \qquad (10)
\end{aligned}
$$

where

$$
h(\mathbf{x}_0) = u_r(\mathbf{x}_0)\left(1 + \frac{R}{V} u'_r(\mathbf{x}_0)\right) \exp\left(-jk\frac{R}{V} u_r(\mathbf{x}_0)\right). \qquad (11)
$$

Then the AT-INSAR phase spectrum $P_p(\mathbf{k})$ is obtained from $I_p(\mathbf{k})$ by calculating the following ensemble average:

$$
\langle I_P(\mathbf{k}) \cdot I_P^*(\mathbf{k}') \rangle = P_P(\mathbf{k}) \delta(\mathbf{k} - \mathbf{k}')
$$

$$
P_P(\mathbf{k}) = \left(\frac{k_i B}{\pi V}\right)^2 \int \exp(-j\mathbf{k}\mathbf{r}) \langle h(\mathbf{x} + \mathbf{r}) h^*(\mathbf{x}) \rangle d\mathbf{r}, \qquad (12)
$$

where

$$
\begin{aligned}
\langle h(\mathbf{x}_0 + \mathbf{r}) h^*(\mathbf{x}_0) \rangle &= \left\langle u_r(\mathbf{x}_0 + \mathbf{r}) u_r(\mathbf{x}_0) \exp\left[-jk\frac{R}{V}(u_r(\mathbf{x}_0 + \mathbf{r}) \right.\right. \\
&\quad \left.\left. - u_r(\mathbf{x}_0))\right]\right\rangle + \frac{R}{V}\left\langle u_r(\mathbf{x}_0 + \mathbf{r}) u_r(\mathbf{x}_0) \right. \\
&\quad \cdot \left(u'_r(\mathbf{x}_0 + \mathbf{r}) + u'_r(\mathbf{x}_0)\right) \exp\left[-jk\frac{R}{V}(u_r(\mathbf{x}_0 + \mathbf{r}) \right. \\
&\quad \left.\left. - u_r(\mathbf{x}_0))\right]\right\rangle + \left(\frac{R}{V}\right)^2 \left\langle u_r(\mathbf{x}_0 + \mathbf{r}) u'_r(\mathbf{x}_0 + \mathbf{r}) \right. \\
&\quad \cdot u_r(\mathbf{x}_0) u'_r(\mathbf{x}_0) \exp\left[-jk\frac{R}{V}(u_r(\mathbf{x}_0 + \mathbf{r}) \right. \\
&\quad \left.\left. - u_r(\mathbf{x}_0))\right]\right\rangle. \qquad (13)
\end{aligned}
$$

[20] The auto-covariance functions occurring in equation (13) can easily be calculated by using the characteristic function method which is described in Appendix A and which has been used before by *Krogstad* [1992] in deriving the nonlinear integral transform for the conventional SAR image spectrum and by *Bao et al.* [1999] in deriving the integral transform for the AT-INSAR phase spectrum.

[21] Thus the final expression for AT-INSAR phase spectrum reads

$$
\begin{aligned}
P_P(\mathbf{k}) &= \left(\frac{k_i B}{\pi V}\right)^2 \int d\mathbf{r} \exp(-j\mathbf{k}\mathbf{r}) \exp\left[\left(\frac{k_x R}{V}\right)^2 (f^u(\mathbf{r}) - f^u(\mathbf{0}))\right] \\
&\quad \times \left\{ \left[f^u(\mathbf{r}) + \left(\frac{k_x R}{V}\right)^2 (f^u(\mathbf{r}) - f^u(\mathbf{0}))^2\right] \left(1 - \frac{\partial^2 f^u(\mathbf{r})}{\partial r^2}\left(\frac{R}{V}\right)^2\right) \right. \\
&\quad + 2j\left(\frac{k_x R^2}{V^2}\right)\left(2f^u(\mathbf{r}) - f^u(\mathbf{0}) + \left(\frac{k_x R}{V}\right)^2 (f^u(\mathbf{r}) - f^u(\mathbf{0}))^2\right) \\
&\quad \cdot \left(\frac{\partial f^u(\mathbf{r})}{\partial r}\right) - \left(\frac{R}{V}\right)^2 \left[1 + \left(\frac{k_x R}{V}\right)^2 (3f^u(\mathbf{r}) - 2f^u(\mathbf{0})) \right. \\
&\quad \left.\left. + \left(\frac{k_x R}{V}\right)^4 (f^u(\mathbf{r}) - f^u(\mathbf{0}))^2\right] \left(\frac{\partial f^u(\mathbf{r})}{\partial r}\right)^2 \right\}, \qquad (14)
\end{aligned}
$$

where

$$
f^u(\mathbf{r}) = \langle u_r(\mathbf{x}_0 + \mathbf{r}) u_r(\mathbf{x}_0) \rangle. \qquad (15)
$$

[22] Equation (14) reduces to equation (11) derived by *Bao et al.* [1999] if in equation (14) the derivatives $\frac{\partial f^u(\mathbf{r})}{\partial r}$ and $\frac{\partial^2 f^u(\mathbf{r})}{\partial r^2}$ are set equal to zero. Note that $u_r(\mathbf{x}_0)$ is defined here as the time average over the period during which the scattering element is viewed by the AT-INSAR.

[23] According to linear wave theory $u_r(\mathbf{x}_0)$ and the sea surface elevation $\zeta(\mathbf{x}_0)$ are linearly related.If we write $\zeta(\mathbf{x}_0)$ in the form

$$
\zeta(\mathbf{x}_0) = \int \zeta(\mathbf{k}) \exp[j\mathbf{k} \cdot \mathbf{x}_0] d\mathbf{k} + c.c., \qquad (16)
$$

then

$$
u_r(\mathbf{x}_0) = \int T_k^u \zeta(\mathbf{k}) \exp(j\mathbf{k}\mathbf{x}_0) d\mathbf{x}_0 + c.c., \qquad (17)
$$

where T_k^u is the range velocity transfer function,

$$
T_k^u = -\omega\left(\sin\theta \frac{k_l}{|k|} + j\cos\theta\right). \qquad (18)
$$

Here ω denotes the frequency of the ocean wave which is related to the ocean wave number k by the dispersion relation, which for deep water waves reads $\omega = \sqrt{|k|g}$, where g is the acceleration of gravity. Thus the auto-covariance function $f^u(\mathbf{r})$ appearing in equation (14) can be written as

$$
f^u(\mathbf{r}) = \frac{1}{2} \int \left(\left|T_{\mathbf{k}}^u\right|^2 F(\mathbf{k}) + \left|T_{-\mathbf{k}}^u\right|^2 F(-\mathbf{k})\right) \exp(j\mathbf{k}\mathbf{r}) d\mathbf{k}, \qquad (19)
$$

where $F(\mathbf{k})$ denotes the ocean wave spectrum defined by

$$
\langle \zeta(\mathbf{k}) \zeta^*(\mathbf{k}') \rangle = \frac{1}{2} F(\mathbf{k}) \delta(\mathbf{k} - \mathbf{k}'). \qquad (20)
$$

4. Nonlinear Integral Transform for the AT-INSAR Amplitude Spectrum

[24] The AT-INSAR amplitude spectrum $P_A(\mathbf{k})$ is obtained from the AT-INSAR amplitude image $I_A(\mathbf{x})$ by first calculating the Fourier transform of equation (8),

$$
\begin{aligned}
I_A(\mathbf{k}) &= (2\pi)^{-2} \int\int \hat{I}_A(\mathbf{x}) \exp(-j\mathbf{k}\mathbf{x}) d\mathbf{x} = (2\pi)^{-2} \int \frac{\sqrt{\pi}}{2} T_0^2 \rho_a \\
&\quad \cdot \exp\left(-\frac{4B^2}{V^2 T_0^2} + \frac{4\rho_a^2 B^2}{\rho_a'^2 V^2 T_0^2}\right) \sigma(\mathbf{x}_0) \times \left[\int\int \exp(-j\mathbf{k}\mathbf{x}) \right. \\
&\quad \left. \cdot \delta(y - y_0) \delta\left(x - x_0 - \frac{R}{V} u_r(\mathbf{x}_0)\right) d\mathbf{x}\right] d\mathbf{x}_0 \\
&= (2\pi)^{-2} \int g(\mathbf{x}_0) \exp(-j\mathbf{k}\mathbf{x}_0) d\mathbf{x}_0, \qquad (21)
\end{aligned}
$$

where

$$g(\mathbf{x}_0) = \frac{\sqrt{\pi}}{2} T_0^2 \rho_a \sigma(\mathbf{x}_0) \exp\left(-\frac{4B^2}{V^2 T_0^2} + \frac{4\rho_a^2 B^2}{\rho_a'^2(\mathbf{x}_0) T_0^2 V^2}\right) \cdot \exp(-jk_x u_r(\mathbf{x}_0)). \tag{22}$$

[25] The AT-INSAR amplitude spectrum $P_A(\mathbf{k})$ is then calculated from $I_A(\mathbf{k})$ in the same way as the AT-INSAR phase spectrum $P_P(\mathbf{k})$ was calculated in the previous section from $I_P(\mathbf{k})$. Again, the auto-covariance functions are calculated by using the characteristic function method as described in Appendix A.

[26] After some tedious but straightforward calculations, we finally obtain the following expression for AT-INSAR phase image spectrum,

$$\begin{aligned} P_A(\mathbf{k}) = {} & (2\pi)^2 \exp\left(k_x^2\left(\frac{R}{V}\right)^2 f^u(\mathbf{0})\right) \int d\mathbf{r} \exp(-j\mathbf{k}\mathbf{r}) \\ & \cdot \exp\left(k_x^2\left(\frac{R}{V}\right)^2 f^u(\mathbf{r})\right) \times \left\{1 + f^R(\mathbf{r}) + jk_x\left(\frac{R}{V}\right)\right. \\ & \cdot \left[f^{Ru}(\mathbf{r}) - f^{Ru}(-\mathbf{r})\right] + \left(k_x\frac{R}{V}\right)^2 \left[\left(f^{Ru}(\mathbf{r}) - f^{Ru}(\mathbf{0})\right)\right. \\ & \left.\left. \cdot \left(f^{Ru}(-\mathbf{r}) - f^{Ru}(\mathbf{0})\right)\right]\right\}, \end{aligned} \tag{23}$$

where

$$f^R(\mathbf{r}) = \frac{1}{2}\int \left(\left|T_{\mathbf{k}}^R\right|^2 F(\mathbf{k}) + \left|T_{-\mathbf{k}}^R\right|^2 F(-\mathbf{k})\right) \exp(j\mathbf{k}\mathbf{r}) d\mathbf{k} \tag{24}$$

$$f^{Ru}(\mathbf{r}) = \frac{1}{2}\int \left(F(\mathbf{k}) T_{\mathbf{k}}^R \left(T_{\mathbf{k}}^u\right)^* + F(-\mathbf{k}) T_{-\mathbf{k}}^u \left(T_{-\mathbf{k}}^R\right)^*\right) \exp(j\mathbf{k}\mathbf{r}) d\mathbf{k}. \tag{25}$$

Here T_{K}^R denotes the transfer function that relates the $\sigma_0(\mathbf{x}_0)$ variation to the ocean wave amplitude in a similar way as $T_{\mathrm{K}}^{\mathrm{u}}$ relates $u_r(\mathbf{x}_0)$ to the ocean wave amplitude (see equation (17)). Since we are here not primarily concerned with the transform for the AT-INSAR amplitude spectrum, we refrain from giving details of this transfer function, which is sometimes also called "real aperture radar transfer function." For details, the reader is referred to the paper by *Hasselmann and Hasselmann* [1991].

5. Quasi-Linear Transform for the AT-INSAR Phase Spectrum

[27] As shown by *Bao et al.* [1999], a quasi-linear approximation for the AT-INSAR phase spectrum can be obtained from the general expression (14) for the case where the nonlinearity parameter is small.

[28] To this end, we first carry out in equation (14) a partial integration with respect to the term $\frac{\partial^2 f^u(\mathbf{r})}{\partial r^2}$ which yields

$$\begin{aligned} P_P(\mathbf{k}) = {} & \left(\frac{k_i B}{\pi V}\right)^2 \int d\mathbf{r} \exp(-j\mathbf{k}\mathbf{r}) \exp\left[\left(\frac{k_x R}{V}\right)^2 \left(f^u(\mathbf{r}) - f^u(\mathbf{0})\right)\right] \\ & \times \left\{\left(\frac{k_x R}{V}\right)^2 \left(f^u(\mathbf{0})\right)^2 + \frac{j}{k_x}\left(\left(\frac{k_x R}{V}\right)^4 f^u(\mathbf{0})^2 - 1\right) \frac{\partial f^u(\mathbf{r})}{\partial r}\right\}. \end{aligned} \tag{26}$$

Then, following *Bao et al.* [1999], we make the following Taylor series expansion and keep only the first two terms:

$$\exp\left[\left(\frac{k_x R}{V}\right)^2 \left(f^u(\mathbf{r}) - f^u(\mathbf{0})\right)\right] = 1 + \left(\frac{k_x R}{V}\right)^2 \left(f^u(\mathbf{r}) - f^u(\mathbf{0})\right). \tag{27}$$

[29] Inserting equation (27) into equation (26), discarding all terms higher than first order in $f^u(\mathbf{r})$, and ignoring a constant term, we obtain the following quasi-linear relationship between the ocean wave spectrum $F(\mathbf{k})$ and the AT-INSAR phase spectrum $P_P(\mathbf{k})$,

$$\begin{aligned} P_P(\mathbf{k}) = {} & \left(\frac{2k_i B}{V}\right)^2 \left(\left|T_{\mathbf{k}}^u\right|^2 \frac{F(\mathbf{k})}{2} + \left|T_{-\mathbf{k}}^u\right|^2 \frac{F(-\mathbf{k})}{2}\right) \\ & \cdot \left(1 - \left(\frac{k_x R}{V}\right)^2 f^u(\mathbf{0}) + \left(\frac{k_x R}{V}\right)^6 \left(f^u(\mathbf{0})\right)^3\right). \end{aligned} \tag{28}$$

Note also that this expression for the quasi-linear transform, which we shall call in the following the first quasi-linear transform, differs from the one derived by *Bao et al.* [1999]. A difference even remains when all terms higher than first order in $f^u(\mathbf{0})$ are neglected.

[30] As shown by *Vachon et al.* [1999], another quasi-linear transform, which in the following we shall call the second quasi-linear transform, can be obtained when the exponential term $\exp\left[\left(\frac{k_x R}{V}\right)^2 \left(f^u(\mathbf{r}) - f^u(\mathbf{0})\right)\right]$ is expanded in a Taylor series in the following way:

$$\exp\left[\left(\frac{k_x R}{V}\right)^2 \left(f^u(\mathbf{r}) - f^u(\mathbf{0})\right)\right] = \exp\left[-\left(\frac{k_x R}{V}\right)^2 f^u(\mathbf{0})\right] \cdot \left[1 + \left(\frac{k_x R}{V}\right)^2 f^u(\mathbf{r})\right]. \tag{29}$$

With this approximation we obtain the following (second) quasi-linear transform relating the ocean wave spectrum $F(\mathbf{k})$ to the AT-INSAR phase spectrum $P_P(\mathbf{k})$:

$$\begin{aligned} P_P(\mathbf{k}) = {} & \left(\frac{2k_i B}{V}\right)^2 \exp\left(-\left(\frac{k_x R}{V}\right)^2 f^u(\mathbf{0})\right) \\ & \cdot \left(\left|T_{\mathbf{k}}^u\right|^2 \frac{F(\mathbf{k})}{2} + \left|T_{-\mathbf{k}}^u\right|^2 \frac{F(-\mathbf{k})}{2}\right). \end{aligned} \tag{30}$$

This quasi-linear transform also differs from the one derived by *Vachon et al.* [1999]. In his equation (16) a factor $(1 - \frac{k_x^2 R^2}{V^2} f^u(\mathbf{0})^2)$ occurs that is missing in our transform (30).

6. Comparison of the Different Integral Transforms

[31] As stated before, our expression (9) relating the ocean wave spectrum to the AT-INSAR phase spectrum contains a term containing the derivative of the radial velocity component term which is not present in the

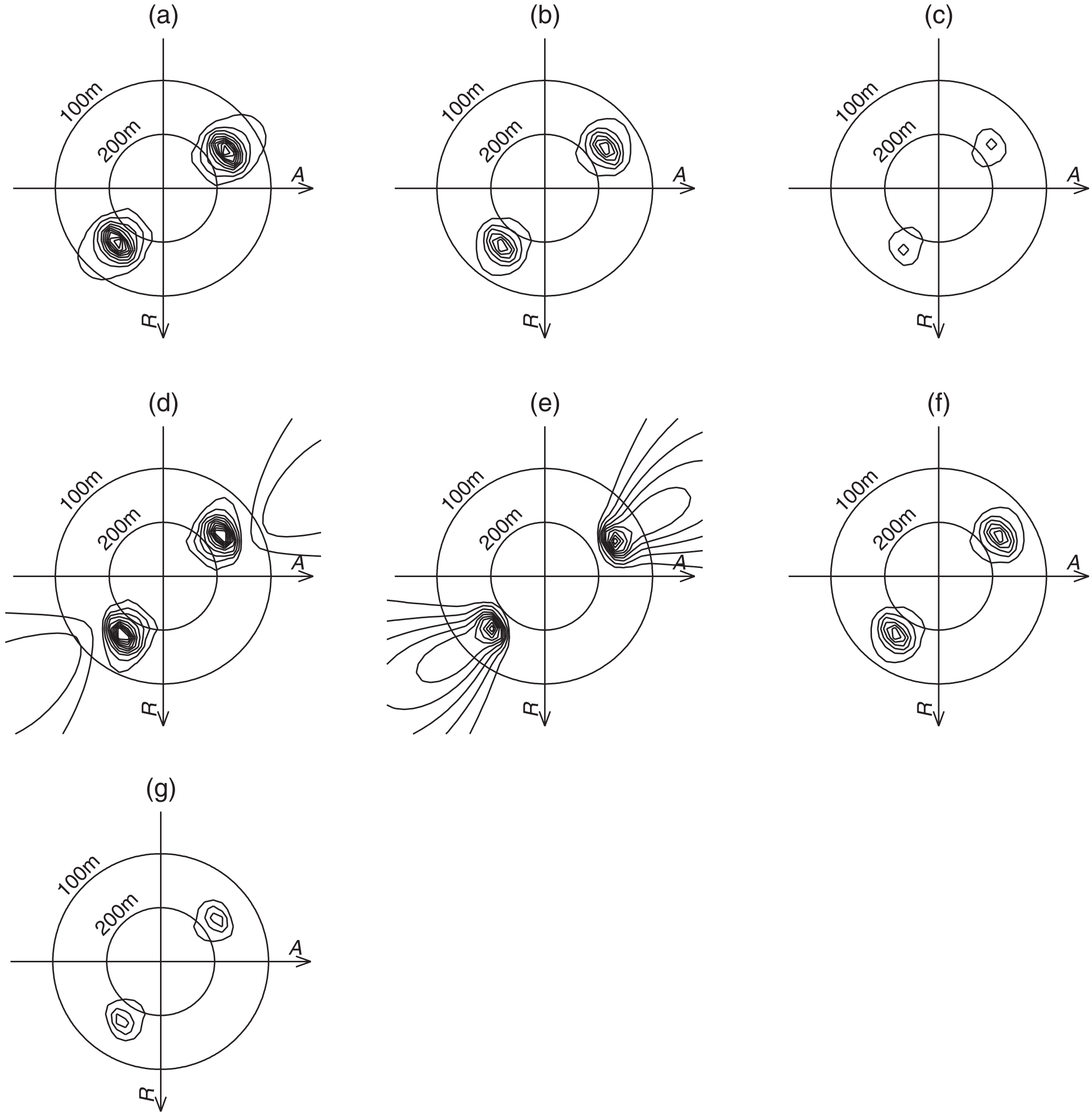

Figure 2. (a) Input ocean wave spectrum (JONSWAP spectrum), (b) AT-INSAR phase spectrum calculated with the nonlinear transform (14), (c) nonlinear AT-INSAR phase spectrum calculated with the nonlinear transform of *Bao et al.* [1999], (d) AT-INSAR phase spectrum calculated with the first quasi-linear transform (28), (e) AT-INSAR phase spectrum calculated with the quasi-linear transform of *Bao et al.* [1999], (f) AT-INSAR phase spectrum calculated with the second quasi-linear transform (30), and (g) AT-INSAR phase spectrum calculated with the second quasi-linear transform of *Vachon et al.* [1999].

corresponding expression (22) of *Bao et al.* [1999]. We now show for one representative example that this term causes quite a difference when calculating the AT-INSAR phase spectrum from the ocean wave spectrum. In this example an ocean wave field having a JONSWAP spectrum is assumed to be imaged by an airborne C-band AT-INSAR.

[32] In the calculations we have used the following AT-INSAR and flight parameters: radar frequency: 5.3 GHz, flight height: 8285 m, incidence angle: 40°, distance between the two antennas (2B): 0.6 m. The JONSWAP spectrum [*Hasselmann et al.*, 1980] used in the calculations has a peak wavelength of 150 m, a peak wave propagation direction with respect to the flight direction of 50°, a significant wave of 1.87 m, and a peak enhancement factor of 3. The wind speed was assumed to be 10.5 m/s.

[33] The results of the calculations obtained by using different transforms are depicted in Figure 2. Figure 2a shows the input JONSWAP spectrum, and Figures 2b and 2c show the AT-INSAR phase spectra calculated with the nonlinear transform (14) derived in this paper and by the nonlinear transform derived by *Bao et al.* [1999], respectively. In Figures 2d and 2e are depicted the AT-INSAR phase spectra calculated with the first quasi-linear transform (28) derived in this paper and with the one derived by *Bao et al.* [1999], respectively. Finally, in Figures 2f and 2g are

depicted the AT-INSAR phase spectra calculated with the second quasi-linear transform (30) derived in this paper and with the corresponding second quasi-linear transform derived by *Vachon et al.* [1999], respectively.

[34] When comparing the AT-INSAR phase spectrum obtained with the nonlinear transform (14) of this paper (Figure 2b) with the one obtained with the nonlinear transform of *Bao et al.* [1999] (Figure 2c) we see that the spectral values obtained with the nonlinear transform (14) of this paper are larger than those obtained with the nonlinear transform of *Bao et al.* [1999]. This implies that the signal-to-noise ratio is also higher.

[35] Furthermore, when comparing the AT-INSAR phase spectra calculated with the two quasi-linear transforms derived in this paper (Figures 2d and 2f) with the AT-INSAR phase spectrum calculated with the nonlinear transform derived in this paper (Figure 2b), we see that the AT-INSAR phase spectrum (Figure 2b) is approximated better by using the second quasi-linear transform (30) than by using the first quasi-linear transform (28). The AT-INSAR phase spectrum calculated with the first quasi-linear transform (Figure 2d) has unrealistic high spectral values for large wave numbers k, which is not the case for the AT-INSAR phase spectrum calculated with the second quasi-linear transform (Figure 2f) because it includes an exponential term $\exp\left[-\left(\frac{k_x R}{V}\right)^2 f^u(\mathbf{0})\right]$, which cuts off the spectral values at high wave numbers.

[36] Finally, when comparing the two AT-INSAR phase spectra obtained with the quasi-linear transforms (28) and (30) of this paper (Figures 2d and 2f) with the corresponding ones obtained by *Bao et al.* [1999] and *Vachon et al.* [1999] (Figures 2e and 2g), respectively, we clearly see differences. This shows that the additional derivative term which is present in our equation (10) is not negligible.

[37] In order to estimate the difference between the simulated AT-INSAR phase spectra obtained by using our transforms and the ones obtained by *Bao et al.* [1999] and *Vachon et al.* [1999], we introduce the parameter κ,

$$\kappa = \frac{\int |P_o(\mathbf{k}) - P_b(\mathbf{k})| d\mathbf{k}}{\int P_o(\mathbf{k}) d\mathbf{k}}.$$

Here $P_o(\mathbf{k})$, $P_b(\mathbf{k})$ denote the AT-INSAR phase spectra calculated with our transforms and with the ones of Bao et al. and Vachon et al., respectively. When comparing the AT-INSAR phase spectra calculated with the nonlinear, the first and second quasi-linear transform derived in this paper and with the corresponding ones of Bao et al. and Vachon et al., we obtain the following values for κ: 1.22, 2.12, and 0.66, respectively. These values for κ confirm our observations made when comparing the AT-INSAR phase spectra depicted in Figures 2a, 2d, and 2f with those depicted in Figures 2c, 2e, and 2g.

7. Conclusion

[38] We have derived a new nonlinear integral transform relating the ocean wave spectrum to the along-track interferometric synthetic aperture radar (AT-INSAR) image spectrum. In addition, we have derived two quasi-linear approximations of the transform relating the ocean wave spectrum to the AT-INSAR phase spectrum. We have found that the nonlinear integral transform for the AT-INSAR amplitude spectrum is essentially the same as the one derived previously by *Hasselmann and Hasselmann* [1991] and *Krogstad* [1992] for the conventional SAR image spectrum. However, the integral transform for the AT-INSAR phase spectrum derived in this paper differs from the one derived by *Bao et al.* [1999]. The difference consists of additional terms containing the auto-covariance function of the derivative and its second derivative of the radial component of the orbital velocity. Also, the two quasi-linear approximations of the nonlinear transform derived in this paper differ from the corresponding quasi-linear approximations derived by *Bao et al.* [1999] and *Vachon et al.* [1999]. Numerical simulations confirm that these additional terms cannot be ignored. In a future study the transforms derived in this paper will be used to compare AT-INSAR phase spectra retrieved from airborne IN-SAR data with measured ocean wave spectra.

Appendix A: The Characteristic Function Method

[39] Let us assume that the random variable $\xi(\mathbf{x})$ describes a stationary Gaussian random process. Then, the auto-covariance function and the variance of $\xi(\mathbf{x})$, respectively, are given by

$$c_{12} = \langle \xi(\mathbf{x})\xi(\mathbf{x}+\mathbf{r}) \rangle \tag{A1}$$

$$c_{11} = \langle \xi^2(\mathbf{x}) \rangle = \langle \xi^2(\mathbf{x}+\mathbf{r}) \rangle. \tag{A2}$$

The characteristic function $T(k_1, k_2)$, which is defined by

$$T(k_1, k_2) = \langle \exp[jk_1\xi(\mathbf{x}) + jk_2\xi(\mathbf{x}+\mathbf{r})] \rangle, \tag{A3}$$

can be written as [see *Bao et al.*, 1999]

$$T(k_1, k_2) = \exp\left[-\frac{1}{2}\left(k_1^2 c_{11} + 2k_1k_2c_{12} + k_2^2 c_{11}\right)\right]. \tag{A4}$$

Then we obtain [*Bao et al.*, 1999]

$$\begin{aligned} \langle \xi(\mathbf{x})\xi(\mathbf{x}+\mathbf{r}) \exp(jk_1\xi(\mathbf{x}) + jk_2\xi(\mathbf{x}+\mathbf{r})) \rangle &= -\frac{\partial^2}{\partial k_1 \partial k_2} T(k_1, k_2) \\ &= \exp\left[-\frac{1}{2}\left(k_1^2 c_{11} + 2k_1k_2c_{12} + k_2^2 c_{11}\right)\right] \\ &\times [c_{12} - (k_1c_{11} + k_2c_{12})(k_1c_{12} + k_2c_{11})]. \end{aligned} \tag{A5}$$

Calculating the partial derivative of (A3) with respect to r yields

$$\frac{\partial T(k_1, k_2)}{\partial r} = \langle jk_2\xi'(\mathbf{x}+\mathbf{r}) \exp(jk_1\xi(\mathbf{x}) + jk_2\xi(\mathbf{x}+\mathbf{r})) \rangle, \tag{A6}$$

and calculating the partial derivatives with respect to k_1 and k_2 of this equation yields

$$\frac{\partial^2}{\partial k_1 \partial k_2}\left(\frac{\partial T(k_1,k_2)}{\partial r}\right) = \langle -\xi'(\mathbf{x}+\mathbf{r})\xi(\mathbf{x})\exp(jk_1\xi(\mathbf{x}) + jk_2\xi(\mathbf{x}+\mathbf{r}))\rangle - \langle jk_2\xi'(\mathbf{x}+\mathbf{r})\xi(\mathbf{x}+\mathbf{r})\xi(\mathbf{x}) \cdot \exp(jk_1\xi(\mathbf{x}) + jk_2\xi(\mathbf{x}+\mathbf{r}))\rangle = \frac{1}{k_2}\frac{\partial}{\partial k_1} \cdot \left(\frac{\partial T(k_1,k_2)}{\partial r}\right) - jk_2\langle \xi'(\mathbf{x}+\mathbf{r})\xi(\mathbf{x}+\mathbf{r})\xi(\mathbf{x}) \cdot \exp(jk_1\xi(\mathbf{x}) + jk_2\xi(\mathbf{x}+\mathbf{r}))\rangle. \tag{A7}$$

Thus

$$\langle \xi'(\mathbf{x}+\mathbf{r})\xi(\mathbf{x}+\mathbf{r})\xi(\mathbf{x})\exp(jk_1\xi(\mathbf{x}) + jk_2\xi(\mathbf{x}+\mathbf{r}))\rangle = \frac{1}{jk_2}\left(\frac{1}{k_2}\frac{\partial}{\partial k_1}\left(\frac{\partial T(k_1,k_2)}{\partial r}\right) - \frac{\partial^2}{\partial k_1\partial k_2}\left(\frac{\partial T(k_1,k_2)}{\partial r}\right)\right) \tag{A8}$$

$$\langle \xi'(\mathbf{x})\xi(\mathbf{x}+\mathbf{r})\xi(\mathbf{x})\exp(jk_1\xi(\mathbf{x}) + jk_2\xi(\mathbf{x}+\mathbf{r}))\rangle = -\frac{1}{jk_1}\left(\frac{1}{k_1}\frac{\partial}{\partial k_2}\left(\frac{\partial T(k_1,k_2)}{\partial r}\right) - \frac{\partial^2}{\partial k_2\partial k_1}\left(\frac{\partial T(k_1,k_2)}{\partial r}\right)\right). \tag{A9}$$

Equation (A6) can also be written as equation (13)

$$\frac{\partial T(k_1,k_2)}{\partial r} = \langle jk_2\xi'(\mathbf{x}+\mathbf{r})\exp(jk_1\xi(\mathbf{x}) + jk_2\xi(\mathbf{x}+\mathbf{r}))\rangle = \langle jk_2\xi'(\mathbf{x})\exp(jk_1\xi(\mathbf{x}-\mathbf{r}) + jk_2\xi(\mathbf{x}))\rangle. \tag{A10}$$

The second partial derivative with respect to r reads

$$\frac{\partial^2 T(k_1,k_2)}{\partial r^2} = \langle k_1k_2\xi'(\mathbf{x})\xi'(\mathbf{x}-\mathbf{r})\exp(jk_1\xi(\mathbf{x}-\mathbf{r}) + jk_2\xi(\mathbf{x}))\rangle = \langle k_1k_2\xi'(\mathbf{x})\xi'(\mathbf{x}+\mathbf{r})\exp(jk_1\xi(\mathbf{x}) + jk_2\xi(\mathbf{x}+\mathbf{r}))\rangle. \tag{A11}$$

Thus we obtain

$$\langle \xi'(\mathbf{x})\xi'(\mathbf{x}+\mathbf{r})\exp(jk_1\xi(\mathbf{x}) + jk_2\xi(\mathbf{x}+\mathbf{r}))\rangle = \frac{1}{k_1k_2}\frac{\partial^2 T(k_1,k_2)}{\partial r^2}. \tag{A12}$$

Differentiating both sides of (A12) with respect to k_1 and k_2 yields

$$\langle \xi'(\mathbf{x})\xi'(\mathbf{x}+\mathbf{r})\xi(\mathbf{x})\xi(\mathbf{x}+\mathbf{r})\exp(jk_1\xi(\mathbf{x}) + jk_2\xi(\mathbf{x}+\mathbf{r}))\rangle = -\frac{\partial^2}{\partial k_1\partial k_2}\left(\frac{1}{k_1k_2}\frac{\partial^2 T(k_1,k_2)}{\partial r^2}\right). \tag{A13}$$

Using the expression (A3) for $T(k_1, k_2)$, we obtain after some tedious, but elementary calculations,

$$\langle \xi'(\mathbf{x})\xi'(\mathbf{x}+\mathbf{r})\xi(\mathbf{x})\xi(\mathbf{x}+\mathbf{r})\exp(jk_1\xi(\mathbf{x}) + jk_2\xi(\mathbf{x}+\mathbf{r}))\rangle = -\Big\{\big[1 - 3k_1k_2c_{12} - k_1^2c_{11} - k_2^2c_{11} + k_1k_2(k_1c_{11} + k_2c_{12}) \cdot (k_1c_{12} + k_2c_{11})\big]\left(\frac{\partial c_{12}}{\partial r}\right)^2 + [c_{12} - (k_1c_{11} + k_2c_{12})(k_1c_{12} + k_2c_{11})] \cdot \frac{\partial^2 c_{12}}{\partial r^2}\Big\}\exp\left[-\frac{1}{2}\left(2k_1k_2c_{12} + k_1^2c_{11} + k_2^2c_{11}\right)\right]. \tag{A14}$$

[40] The equations (A5), (A8), (A9), and (A14) are the fundamental equations for the characteristic function method used in the derivation of the nonlinear integral transforms. If we replace in those equations k_1 and k_2 by $\frac{k_xR}{V}$ and $-\frac{k_xR}{V}$, respectively, and $\xi(\mathbf{x})$ by $u_r(\mathbf{x}_0)$, we obtain equation (13).

[41] **Acknowledgments.** This work was partly supported by the National Natural Science Foundation of the People's Republic of China through the grants 49986001 and 40276050, and by a cooperation exchange project between the Chinese Academy of Sciences and the German Max-Planck Society through grant KZCX2-202. The authors thank the two anonymous referees for helpful suggestions.

References

Alpers, W., and K. Hasselmann, The two-frequency microwave technique for measuring ocean-wave spectra from an airplane or satellite, *Boundary Layer Meteorol.*, *13*, 215–230, 1978.

Alpers, W., and C. L. Rufenach, The effect of orbital motion on synthetic aperture radar imagery of ocean waves, *IEEE Trans. Antennas Propag.*, *27*, 685–690, 1979.

Alpers, W., D. B. Ross, and C. L. Rufenach, On the detectability of ocean surface waves by real and synthetic aperture radar, *J. Geophys. Res.*, *86*, 6481–6498, 1981.

Bao, M., C. Brüning, and W. Alpers, Simulation of ocean waves imaging by an along-track interferometric synthetic aperture radar, *IEEE Trans. Geosci. Remote Sens.*, *35*, 618–631, 1997.

Bao, M., W. Alpers, and C. Brüning, A new nonlinear integral transform relating ocean wave spectra to phase image spectra of an along-track interferometric synthetic aperture radar, *IEEE Trans. Geosci. Remote Sens.*, *37*, 461–466, 1999.

Brüning, C., W. Alpers, and K. Hasselmann, Monte-Carlo simulation studies of the nonlinear image of a two-dimensional surface wave field by SAR, *Int. J. Remote Sens.*, *11*, 1695–1727, 1990.

Goldstein, R. M., and H. A. Zebker, Interferometric radar measurements of ocean surface currents, *Nature*, *328*, 707–709, 1987.

Goldstein, R. M., T. P. Barnett, and H. A. Zebker, Remote sensing of ocean currents, *Science*, *246*, 1282–1285, 1989.

Hasselmann, D. E., M. Dunckel, and J. A. Ewing, Directional wave spectra observed during JONSWAP 1973, *J. Phys. Oceanogr.*, *10*, 1264–1280, 1980.

Hasselmann, K., and S. Hasselmann, On the nonlinear mapping of an ocean wave spectrum into a synthetic aperture radar image spectrum and its inversion, *J. Geophys. Res.*, *96*, 10,713–10,729, 1991.

Hasselmann, K., R. K. Raney, W. J. Plant, W. Alpers, R. A. Shuchman, D. R. Lyzenga, C. L. Rufenach, and M. J. Tucker, Theory of synthetic aperture radar ocean imaging: A MARSEN view, *J. Geophys. Res.*, *90*, 4659–4686, 1985.

Hasselmann, S., C. Brüning, K. Hasselmann, and P. Heimbach, An improved algorithm for the retrieval of ocean wave spectra from synthetic aperture radar image spectra, *J. Geophys. Res.*, *101*, 16,615–16,629, 1996.

Heimbach, P., S. Hasselmann, and K. Hasselmann, Statistical analysis and intercomparison of WAM model data with global ERS-1 SAR wave mode spectral retrievals over 3 years, *J. Geophys. Res.*, *103*, 7931–7977, 1998.

Krogstad, H. E., A simple derivation of Hasselmann's nonlinear ocean-synthetic aperture radar transform, *J. Geophys. Res.*, *97*, 2421–2425, 1992.

Lyzenga, D. R., and J. R. Bennett, Estimation of ocean wave spectra using two-antenna SAR systems, *IEEE Trans. Geosci. Remote Sens.*, *29*, 463–465, 1991.

Marom, M., R. M. Goldstein, E. B. Thornton, and L. Shemer, Remote sensing of ocean wave spectra by interferometric synthetic aperture radar, *Nature*, *345*, 793–795, 1990.

Marom, M., L. Shemer, and E. B. Thornton, Energy density directional spectra of a near-shore wave field measured by interferometric synthetic aperture radar, *J. Geophys. Res.*, *96*, 22,125–22,134, 1991.

Shemer, L., An analytical presentation of the monochromatic ocean wave image by a regular or an interferometric synthetic aperture radar, *IEEE Trans. Geosci. Remote Sens.*, *33*, 1008–1013, 1995.

Shemer, L., and E. Kit, Simulation of an interferometric synthetic aperture radar imagery of an ocean system consisting of a current and a monochromatic wave, *J. Geophys. Res.*, *96*, 22,063–22,073, 1991.

Swift, C. F., and L. R. Wilson, Synthetic aperture radar imaging of ocean waves, *IEEE Trans. Antennas Propag.*, *27*, 725–729, 1979.

Vachon, P. W., J. W. M. Campbell, A. L. Gray, and F. W. Dobson, Validation of along-track interferometric SAR measurements of ocean surface waves, *IEEE Trans. Geosci. Remote Sens.*, *37*, 150–162, 1999.

Zilman, G., and L. Shemer, An exact analytic representation of a regular or interferometric SAR image of ocean swell, *IEEE Trans. Geosci. Remote Sens.*, *37*, 1015–1022, 1999.

W. Alpers, Institute of Oceanography, University of Hamburg, Bundestrasse 55, D-20146 Hamburg, Germany. (alpers@ifm.uni-hamburg.de)

Y. He, Institute of Oceanology, Chinese Academy of Sciences, 7 Nanhai Road, Qingdao 266071, China. (heyj@ms.qdio.ac.cn)